Rapid Generation of Single-Tumor Spheroids for High-Throughput Cell Function and Toxicity Analysis

ANDREA IVASCU and MANFRED KUBBIES

Spheroids are widely used in biology because they provide an in vitro 3-dimensional (3D) model to study proliferation, cell death, differentiation, and metabolism of cells in tumors and the response of tumors to radiotherapy and chemotherapy. The methods of generating spheroids are limited by size heterogeneity, long cultivation time, or mechanical accessibility for higher throughput fashion. The authors present a rapid method to generate single spheroids in suspension culture in individual wells. A defined number of cells ranging from 1000 to 20,000 were seeded into wells of poly-HEMA–coated, 96-well, round- or conical-bottom plates in standard medium and centrifuged for 10 min at 1000*g*. This procedure generates single spheroids in each well within a 24-h culture time with homogeneous sizes, morphologies, and stratification of proliferating cells in the rim and dying cells in the core region. Because a large number of tumor cell lines form only loose aggregates when cultured in 3D, the authors also performed a screen for medium additives to achieve a switch from aggregate to spheroid morphology. Small quantities of the basement membrane extract Matrigel, added to the culture medium prior to centrifugation, most effectively induced compact spheroid formation. The compact spheroid morphology is evident as early as 24 h after centrifugation in a true suspension culture. Twenty tumor cell lines of different lineages have been used to successfully generate compact, single spheroids with homogenous size in 96-well plates and are easily accessible for subsequent functional analysis. (*Journal of Biomolecular Screening* 2006:922-932)

Key words: tumor, spheroid, cell aggregate, Matrigel (rBM), apoptosis, high-throughput screening

INTRODUCTION

MONOLAYER CELL CULTURES insufficiently reflect the physiological response pattern of the in vivo situation because of fundamental geometric differences between 2-dimensional (2D) cultures and 3-dimensional (3D) solid tumors. A 3D architecture of tumor cells needs to be generated in vitro to simulate the multicellular microenvironment when investigating the tumor cell physiology and response to therapeutic agents. Multicellular tumor spheroids have been widely used as an in vitro 3D model over the past decades to study tumor cell proliferation, apoptosis, differentiation, gene expression, and metabolism in a multicellular context. Tumor spheroids are considered an improved in vitro model to mimic biological properties of micrometastases and vessel distal regions of tumors because they retain the architecture and many morphological and physiological characteristics of their tumor counterparts.[1,2]

Roche Pharmaceutical Research Oncology, Penzberg, Germany.

Received Jan 12, 2006, and in revised form Jul 7, 2006. Accepted for publication Jul 11, 2006.

Journal of Biomolecular Screening 11(8); 2006
DOI:10.1177/1087057106292763

Tumor cells in spheroids show a higher degree of morphological[3-5] and functional[6-9] differentiation than cells grown in monolayer culture. They also display growth kinetics,[10,11] metabolic rates, and resistance to radiotherapy and chemotherapy similar to tumor cells in vivo.[12-16] The increased cell-cell and cell-matrix contacts in compact spheroids not only alter gene expression patterns[17,18] and resistance to antineoplastic treatment but also limit the diffusion of nutrients, oxygen, and waste products into and out of the spheroids.[2] This gives rise to a more stratified composition, with the rim of spheroids consisting of proliferating cells, followed by a layer of quiescent cells in the middle and necrotic cells in the center of the spheroid.[11] A similar cellular heterogeneity is present in nonvascularized tumor regions.[1,19]

Because monolayer-based high-throughput (HT) systems have only a limited predictive value for the in vivo efficacy of antineoplastic compounds, the implementation of the spheroid model in the drug discovery process may improve the predicted activity of new cancer drugs in cell-based screening assays.[20] Several approaches have been developed to enable drug screening using spheroids: confocal microscopy to measure drug or antibody permeation into the spheroid,[20,21] electrochemical microscopy to measure the respiratory activity,[22] image cytometry to quantify lactate dehydrogenase activity as a marker for

cell viability,[23] or biosensors composed of spheroids monitoring physiological alterations by impedance measurements.[24] However, the use of spheroids in an HT fashion in oncology research requires a standardized protocol that rapidly generates spheroids of homogenous size with similar diffusion gradients and cell physiology in a plate format that is easily accessible for subsequent biochemical or cell analysis.

Various culture techniques are used to generate spheroids.[25] In the liquid-overlay technique, trypsinized cells are placed on dishes covered with a thin film of agar.[26] Because the coating prevents cell attachment to the dish, cells can grow only in 3D, and individual cells give rise to aggregates or spheroids. In the spinner flask[27] and the gyratory rotation technique,[28] trypsinized cells are placed in a culture vessel with a magnetic stirrer, inhibiting cell attachment to the substrate and favoring cell-cell adhesion. In a more recently developed technique, spheroids are grown in a hanging drop of an inverted microplate.[29] However, these methods are limited by either long cultivation time, formation of unequal-size spheroids, or difficult mechanical accessibility. In addition, in suspension cultures, many tumor cell lines grow poorly in 3D as compact spheroids.[1,20] They form loose aggregates of cells only, an architecture that is significantly different from the in vivo tumor morphology.

To use tumor spheroids in an HT format, we developed a simple protocol for rapid production of homogenous multicellular tumor spheroids even from aggregate-forming cell types. In this study, we demonstrate that single, compact spheroids with homogeneous sizes can be generated rapidly and in large scale in 96-well microplates as suspension cultures. Moreover, this technique is applicable to a large variety of tumor cell lines.

MATERIALS AND METHODS

Cell culture

The following breast cancer cell lines were applied to establish a protocol for rapid spheroid generation in a 96-well format: MDA-MB-231 (ATCC HTB 26), MDA-MB-468 (ATCC HTB 132), SK-BR-3 (ATCC HTB 30), T-47D (ATCC HTB 133), MCF7 (ATCC HTB 22), MCF7-ADR (Balcer-Kubiczek et al.), and MDA-MB-435S (ATCC HTB 129, which might be of melanoma origin if spontaneous transdifferentiation event can be excluded). In addition, the optimal protocol was tested in the following cell lines: UO-31 (NCI), HEK 293 (ATCC CRL-1573), SK-OV-3 (ATCC HTB 77), IGR-OV-1 (NCI), NCI-H460 (HTB 177), NCI-H322M (NCI), A549 (ATCC CCL 185), PC-3 (ATCC CRL 1435), LNCaP (ATTC CRL 1740), Colo 205 (ATCC CCL 222), SW-620 (CCL 227), HCT-15 (ATCC CCL 225), and HepG2 (ATCC HB 8065). All cells were cultured in RPMI 1640 (PAA Laboratories GmbH, Innsbruck, Austria) with 10% fetal calf serum (FCS; Gibco-BRL, Karlsruhe, Germany) and 2 mM L-glutamine (Gibco-BRL), with the exception of SK-BR-3 cells, which were cultivated in McCoy's 5A (Gibco-BRL) with the same medium supplements.

Screen for medium additives to induce spheroid formation from aggregates

MDA-MB-231 cells grown as a monolayer were detached with Accutase (PAA Laboratories GmbH), and 5000 cells were distributed into single wells of round-bottom, 96-well plates (Corning Inc., New York, NY). To prevent cell attachment, the plates were precoated with 50 µl 0.5% poly-HEMA (Polysciences, Eppelheim, Germany) in 95% ethanol and air dried at 37° C for 3 days prior to use. The cells were pelleted at the bottom of the wells by centrifugation of the plates at 1000*g* for 10 min using a swinging bucket Eppendorf 5810 centrifuge (Eppendorf AG, Hamburg, Germany). For optimal spheroid formation, the following additives were tested: reconstituted basement membrane (rBM; BD Biosciences, Bedford, MA) at 5, 15, 25, 35, and 75 µl/ml and collagen type I (Roche Diagnostics GmbH, Mannheim, Germany), collagen type IV (Fluka, Taufkirchen, Germany), fibronectin (Roche Diagnostics GmbH), and laminin (Roche Diagnostics) at 1, 5, 10, 25, 100, and 500 µg/ml. Heparan sulphate proteoglycane (Sigma-Aldrich, Deisenhofen, Germany) and chondroitin sulphate (Sigma-Aldrich) were tested at 1, 5, and 10 µg/ml. The single additives or combinations were added after centrifugation directly into the wells. The plates were incubated under standard cell culture conditions at 37° C, 7% CO_2 in humidified incubators.

Generation of spheroids

Cells grown as a monolayer were detached with Accutase to generate a single-cell suspension. The cell number was determined using a CASY particle counter instrument (Schaerfe-Systems, Reutlingen, Germany). The cell suspension was diluted to 2.5×10^4 (for 5000 cells per spheroid) or 5×10^4 (for 10,000 cells per spheroid) cells per milliliter of ice-cold medium. The rBM was thawed on ice overnight and added at a final concentration of 2.5% with ice-cold pipette tips to the cell suspension. A volume of 200 µl of this cell suspension was added to each well of a poly-HEMA–coated 96-well plate with a round or conical bottom (Nunc, Roskilde, Denmark). The spheroid formation was initiated by centrifugation of the plates at 1000*g* for 10 min. The plates were incubated under standard cell culture conditions at 37° C, 7% CO_2 in humidified incubators.

Assessment of spheroid cell apoptosis

Spheroids were generated from 8 breast cancer cell lines using 10,000 cells per spheroid. All cell lines except MCF7 and T-47D were grown in the presence of 2.5% rBM. For apoptosis analysis, the spheroids were transferred into a 96-well conical-bottom plate, washed once with phosphate-buffered saline

(PBS), resuspended in Accutase solution, and incubated at 37° C. Every 5 min, the spheroids were resuspended by pipetting, and dissociation was almost complete within 15 to 20 min. The single-cell suspensions from the 8 spheroids were pooled, and cells were stained with annexin-V-fluos and propidium iodide in the prescence of supplemented 2 mM $CaCl_2$ (annexin-V-fluos staining kit; Roche Diagnostics GmbH). The fluorescence from 10,000 cells was acquired using a fluorescence-activated cell sorting (FACS) scan instrument (Becton Dickinson, San Jose, CA). Quadrant statistics was applied on the dot plots, with the number of viable cells located in the lower-left quadrant. To determine the absolute cell number of viable cells within growing spheroids, MDA-MB-231 spheroids were dissociated as described above. The number of total cells from 3 individual spheroids were counted using a CASY particle counter instrument and multiplied with the percentage of viable cells of the same spheroid as determined from the annexin-V assay.

Localization of cell death within spheroids

MDA-MB-231 spheroids were generated from 10,000 cells with the addition of 2.5% rBM. The spheroids were transferred into a 96-well, round-bottom plate and resuspended in 200 µl RPMI without rBM to reduce unspecific binding of propidium iodide (PI; Sigma-Aldrich) to the rBM. The spheroids were stained within the wells with 1 µg/ml PI for 3 h. The localization of PI-positive stained cells within the spheroids was assessed by phase contrast and PI fluorescence microscopy of superimposed images.

Hematoxylin and eosin stain of spheroid slices

MDA-MB-231 spheroids generated from 10,000 cells in the presence of 2.5% rBM prior staining were cultivated for 3 days, washed once in PBS, fixed overnight with 4% formalin (Merck, Darmstadt, Germany), and embedded in paraffin. Microtone (Leica, SM, 2000R) sections of 5 µm were placed on SuperFrost glass slides (Menzel, Braunschweig, Germany) and allowed to dry for 2 h at 37° C. The sections were deparaffinized by 3 changes of xylol for 5 min, rehydrated by 2 changes of 100% ethanol, followed by 80% ethanol and 2 washes in 70% ethanol for 2 min each. After a short single rinse in distilled water, the sections were stained for 20 min in Mayer's hematoxylin (Merck) and placed for 20 min under running tap water. Sections were counterstained with eosin (Merck) for 4 min, dehydrated by 2 changes of 70% ethanol, followed by 1 change to 80% ethanol, 1 in 100% ethanol for 2 min each, and 2 changes of xylol for 5 min. The slides were mounted in Eukitt (KO Kindler, Germany), and spheroid sections were assessed by bright field microscopy.

Immunoblotting of cell membrane proteins

MDA-MB-231 spheroids were generated in the presence of 2.5% rBM and harvested after 1 and 10 days. Spheroids from one 96-well plate were pooled, washed twice with ice-cold PBS, and solubilized in 200 µl lysis buffer (50 mM HEPES, pH 7.5, 150 mM NaCl, 1.5 mM $MgCl_2$, 100 mM NaF, 10 mM NaPyrophosphat, 1 mM EDTA, 10% glycerol, 1% Triton X100, 0.4 mM Na_3VO_4, 10 µM PMSF, 10 µg/ml aprotinin). Lysates were shaken for 30 min at 4° C and centrifuged for 15 min at 15,000 rpm. The protein concentration was determined using the BCA protein assay kit (Pierce, Rockford, IL). A total of 20 µg protein extract was mixed with 4× loading buffer (Invitrogen, Carlsbad, CA), resolved on a 4% to 12% denaturing Bis-Tris Gel (Invitrogen), and transferred with 50 mM Tris, 40 mM glycin, 20% methanol, and 0.04% sodium dodecyl sulfate in a semidry blot chamber (BioRad Laboratories, Hercules, CA) for 1 h and 120 mA (for 117 cm^2) onto a nitrocellulose membrane. Immunostaining of the proteins was performed with the LumiLight^{PLUS} Western Blotting Kit (Roche Diagnostics) according to the manufacturer's instructions. Human integrin β1, claudin 4, and β-actin were probed using anti-integrin β1 (BD Biosciences), anticlaudin-4 (Zymed Laboratories, South San Francisco, CA), and anti-β-actin (Abcam, Cambridge, UK)–specific antibodies.

Determination of spheroid growth kinetics

MDA-MB-231 spheroids were generated from 1000 and 10,000 cells in the presence of 2.5% rBM. Monolayer cultures were generated by seeding each 5×10^4 cells into single wells of a 6-well plate. 5-bromo-2-deoxy-uridine (BrdU; Sigma-Aldrich) was added at 8×10^{-5} M to cell cultures. Spheroids were harvested daily up to 10 days, monolayer control cultures were harvested daily up to 3 days, and BrdU was added for the final 24 h at each time point to determine the nonproliferating, resting G1 cells and dividing cells. The harvested cells were centrifuged and resuspended in 500 µl DNA staining buffer (100 mM Tris-HCl, pH 7.4, 0.9% NaCl, 1 mM $CaCl_2$, 0.5 mM $MgCl_2$, 0.2% bovine serum albumin, 0.1% NP40) supplemented with 60 U/ml RNAse (Calbiochem, Darmstadt, Germany). The buffer lysed the cytoplasmic but not the nucleus membrane. The nuclei were stained with 1.5 µg/ml Hoechst 33258 (Sigma-Aldrich) for 15 min on ice in the dark and counterstained with 2 µg/ml PI for another 15 min. The DNA fluorescence of the nuclei was recorded from 10,000 cells using a FACS LSR instrument (Becton Dickinson). Region-of-interest gating was applied to identify noncycling G1 cells and slowly cycling and rapidly dividing cells (see regions R1, R2, and R3 in **Fig. 5**).

Microscopy

The morphology of the spheroids was assessed and recorded using an Axiovert 135 Microscope (Zeiss, Jena, Germany) and a 5× objective. Pictures were taken with a Xillix Microimager Camera (Xillix Technology Corporation, Richmond, Canada) using the Open Lab 2.2.5 Software (Improvision, Coventry, UK).

The size of the spheroids was analyzed using the calibration software analysis tools and an objective calibration slide (Zeiss).

RESULTS

Single spheroid formation in 8 breast cancer cell lines

To generate homogenous 3D culture spheroids from tumor cells in a screening format, we centrifuged 5000 cells in 96 round- or conical-bottom plates precoated with poly-HEMA to prevent cell attachment. The plates were centrifuged for 10 min at 1000*g*. During the centrifugation, all cells within the well are pelleted at the bottom of the plate. This ensures equal cell numbers for initiation of the formation of a single spheroid in each well of a 96-well plate. We evaluated a panel of 8 breast cancer cell lines according to their ability to form spheroids in microplates. As shown in **Figure 1**, 3 cell lines, MCF7, T-47D, and MDA-MB-435, form multicellular spheroids within 24 h of cultivation. The spheroids formed by MCF7 and T-47D cells are highly compact (**Fig. 1A, B**), whereas MDA-MB-435 cells are incorporated into a spheroid with loosely associated cells at the periphery (**Fig. 1C**). The adriamycin-resistant cell line derived from MCF7 and MCF7-ADR reaches the spheroid morphology after 48 h of cultivation (**Fig. 1D**). Four cell lines, namely, MDA-MB-231, MDA-MB-468, SK-BR-3, and MDA-MB-361, form only loose aggregates of cells after 24 h (**Fig. 1E-H**). The cell-cell contacts established by these cultures are weak, and the aggregates can be easily dispersed mechanically by pipetting. This morphology observed initially did not change within 14 days of cultivation. We defined these latter cultures as loose aggregates in contrast to spheroids formed by MCF7 or T-47D cells.

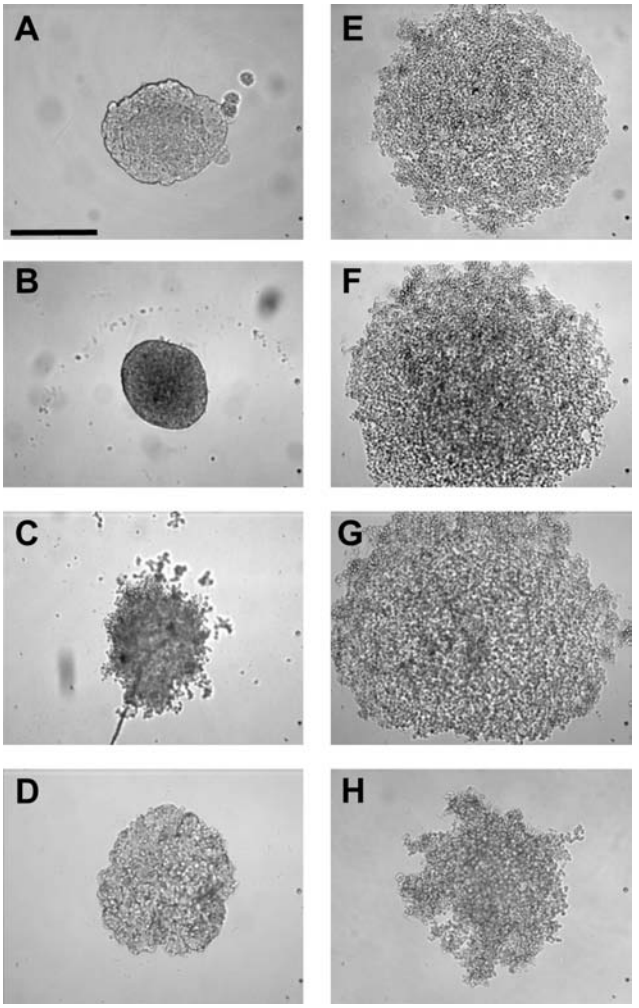

FIG. 1. Rapid formation of spheroids or aggregates of different breast cancer cell lines using poly-HEMA–coated 96-well, round-bottom plates (5000 cells/well, 24-h culture period; exception: 48 h for MCF7-ADR). (**A**) MCF7, (**B**) T-47D, (**C**) MDA-MB-435 (might be of melanoma origin in case that transdifferentiation event can be excluded), (**D**) MCF7-ADR, (**E**) MDA-MB-231, (**F**) MDA-MB-468, (**G**) SK-BR-3, and (**H**) MDA-MB-361. Size of black bar = 500 µm.

Medium additives for induction and time kinetics of spheroid formation

To achieve a tighter spheroid-like 3D morphology, we performed a screen for medium additives using the aggregate-forming cell line MDA-MB-231. Fibronectin, laminin, and collagen type IV were tested at concentrations from 1 to 500 µg/ml, and heparan sulphate proteoglycane and chondroitin sulphate were applied at concentrations ranging from 1 to 10 µg/ml. Any single component added to cell aggregates did not alter the aggregate morphology up to 14 days of culture (representative examples are shown in **Fig. 2A-D**). A preparation of collagen I from rat tail tendon partially increased the intercellular contacts of the MDA-MB-231 3D culture, with some evidence of tight local packaging (**Fig. 2E**). This effect was observed at and above a concentration of 10 µg/ml. A combination of 2, 3, or all components led to a partial compaction of the aggregate only in the presence of collagen I (data not shown). The optimal compaction status was achieved with liquid rBM as additive. At a concentration of 2.5% rBM, all cells were incorporated in 1 distinct spheroid with a round geometry (**Fig. 2F**). Formation and compaction were completed after 24 h of culture time. Lower concentrations of rBM did not ensure the incorporation of all cells into the spheroid, and higher concentrations impaired the round geometry of the spheroids.

Figure 3 shows the kinetics in spheroid formation of MDA-MB-231 cells without (**A-D**) and in the presence (**E-H**) of liquid reconstituted basement membrane (rBM). After the 10-min centrifugation step, all cells within the well are incorporated into 1 flat pellet of cells (**Fig. 3A, E**). Three hours later, some degree of compaction becomes evident in both assay formats (**Fig. 3B, F**). Without rBM, no further tightening of the aggregates can be observed after 6 and 24 h (**Fig. 3C, D**). In contrast, the addition of rBM induces an ongoing compaction in MDA-MB-231

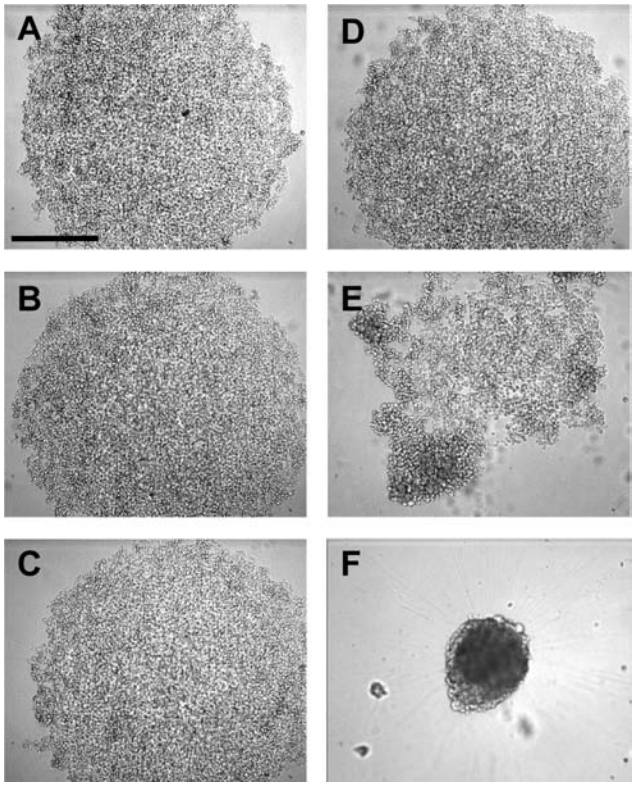

FIG. 2. Medium additive-dependent formation of MDA-MB-231 spheroids using poly-HEMA–coated, round-bottom, 96-well plates (5000 cells/well, 24-h culture period). (**A**) No additive, (**B**) fibronectin 10 μg/ml, (**C**) laminin 10 μg/ml, (**D**) heparan sulfate proteoglycane 20 μg/ml, (**E**) collagen I 10 μg/ml, and (**F**) reconstituted basement membrane (2.5% rBM). Size of black bar = 500 μm.

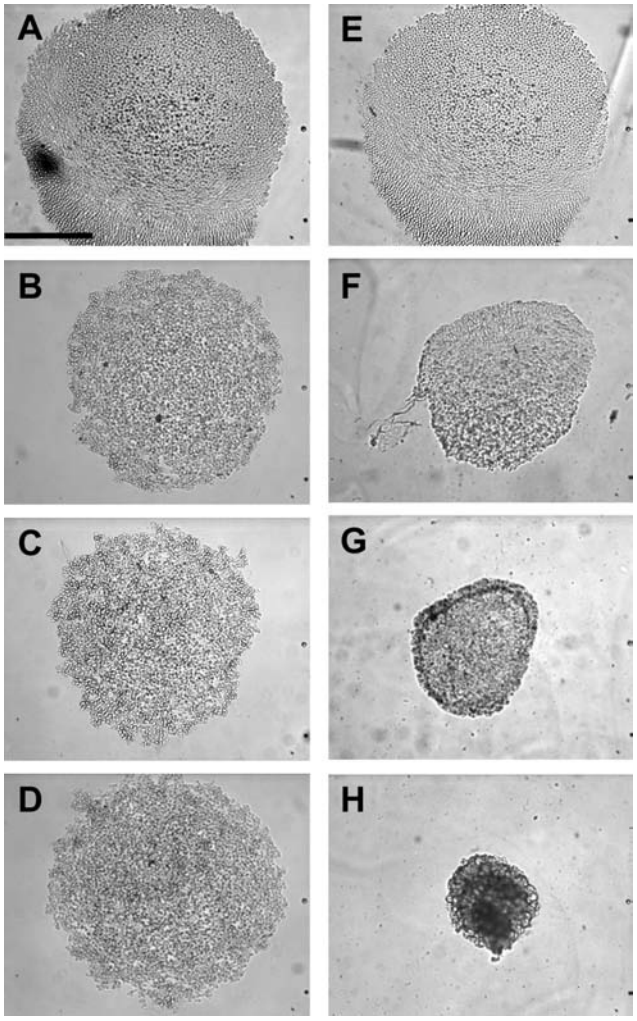

FIG. 3. Kinetics of MDA-MB-231 spheroid formation using poly-HEMA–coated, round-bottom, 96-well plates (5000 cells/well, 24-h culture period). Aggregate formation in the absence of reconstituted basement membrane (rBM) after 0, 3, 6, and 24 h (**A-D**). Spheroid formation in the presence of 2.5% rBM after 0, 3, 6, and 24 h (**E-H**). Size of black bar = 500 μm.

aggregates, and after 6 h, a tight cell association can be observed in the presence of rBM (**Fig. 3G**). The forming spheroids show a reduction in diameter of almost 50% of the initial aggregate, and after 24 h, the spheroid formation is completed (**Fig. 3H**). The spheroids retain their tight structure and do not disintegrate by pipetting as do their aggregate counterparts.

Characteristics of MDA-MB-231 spheroids induced by rBM additive

To investigate the effect of rBM on the tightness of the cell packaging in spheroids, we examined histological sections of MDA-MB-231 spheroids grown for 3 days in culture. **Figure 4A** shows an H&E stain from the rim section of the top of a spheroid. It is evident that the cell density of MDA-MB-231 cells is high in this region. **Figure 4B** displays an H&E stain of a middle section of a spheroid encompassing rim and center structures. It is obvious that the rim of the spheroid consists of about 4 to 6 cell layers of tightly packed cells. Toward the center, the cells are less densely packed, most probably because of onging cell death (see also **Fig. 8A, B**).

To evaluate the similarity of cell-cell adhesions of spheroids generated rapidly with the centrifugation technique compared to spheroids grown from a few cells over extended periods of time, we investigated the expression patterns of adhesion and tight junction proteins of 24-h spheroids derived from 10,000 cells with 10-day-old spheroids derived from 1000 cells: integrin β1 and claudin 4. The Western blot in **Figure 4C** reveals that there was no difference in the expression patterns of these proteins in the different culture setups (loading control β-actin).

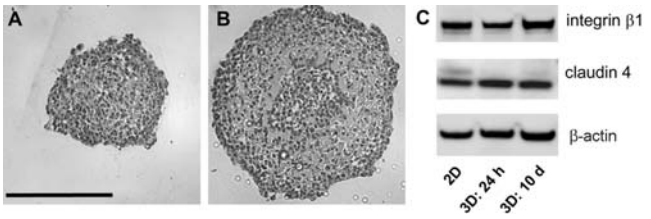

FIG. 4. Cell tightness and interaction analysis of MDA-MB-231 spheroids. H&E stain of spheroid slices from the top (rim area, **A**) and the middle (rim and core area, **B**) of a 3-day spheroid generated from 10,000 cells in the presence of reconstituted basement membrane (bar = 250 μm). (**C**) Expression of the adhesion molecule integrin β1 and the tight junction protein claudin 4 in spheroids grown for 24 h from 10,000 cells and for 10 days from 1000 cells. An approximately 80% confluent MDA-MB-231 monolayer culture served as positive control.

Growth kinetics of MDA-MB-231 spheroids

To determine whether cells in spheroids generated by centrifugation exhibit a decreased proliferation rate compared to monolayer culture, we analyzed the growth kinetics of up to 10 days using the flow cytometric BrdU/Hoechst quenching technique.[30] A 24-h BrdU pulse at the end of the culture period was applied to identify proliferating cells by BrdU-dependent Hoechst dye quenching. Region 1 of the dot plots in **Figure 5** reveals that in monolayer culture, only 0.8% of the cells did not exit the G1 phase. On the contrary, in spheroids generated from 10,000 cells and grown for 1, 5, and 10 days, the noncycling G1-phase fractions increased from 26.4% to 67.7% and 76.0%, respectively. For spheroids generated by centrifugation with only 1000 cells, the number of noncycling G1-phase cells is slightly lower, indicating improved nutrient and growth factor supply (1-, 5-, and 10-day spheroids: 26.6%, 43.3%, and 66.1% noncycling cells, respectively; FACS plots not shown). The number of cells having divided within 24 h of the BrdU pulse were gated in R3 of **Figure 5**. The quantiative results shown at the bottom of **Figure 5** indicate a rapid drop in dividing cells within the first 2 days of the spheroid culture. In subconfluent monolayer cultures, the proportion of dividing cells from day 1 through day 3 is between 55% and 65% of the total population. Most important, the BrdU/Hoechst-PI dot plots reveal that the dying cell fractions, located primarily in the center of the spheroids (see **Fig. 8**), originate from the growth-arrested, noncycling G1-phase population as evident by the sub-G1 lane in **Figure 5** (see arrows).

Generation of homogenous spheroids from aggregates

We tested the ability of rBM to promote spheroid formation in a variety of breast cancer cell lines that failed to establish a compact morphology when grown in 3D suspension culture after 24 h (**Fig. 1E-H**). Like in MDA-MB-231 cells (**Fig. 3**), the addition of liquid rBM to the culture medium induced spheroid formation from aggregates of MDA-MB-468 and SK-BR-3 cells (**Fig. 6A, B**). The 3D structure of MDA-MB-435 and MDA-MB-361 cells also became tighter in the presence of rBM (**Fig. 6C, D**). The microscopic inspection of spheroid morphology in round- versus conical-bottom 96-well plates revealed that the overall density was slightly higher for some cell lines in conical-bottom wells (data not shown).

To evaluate the homogeneity of single-well spheroids, we quantitated their sizes by microscopic analysis. Spheroids were generated from 8 breast cancer cell lines using 96-well, conical-bottom, poly-HEMA–coated plates. Five thousand cells were centrifuged in RPMI 1640 with 10% FCS and 2.5% rBM, and spheroid size was analyzed after a 24-h culture period. **Figure 7** shows typical examples of 6 spheroids each generated from MDA-MB-231 and MCF7 cells, respectively. All spheroids are regular in shape, display a uniform round geometry, and exhibit a narrow size variation. The spheroid volumes were calculated using the geometric mean of 2 orthogonal diameters. Depending on the cell line, the volume of the spheroids formed 24 h after centrifugation from 5000 cells per well ranged from 0.039 to 0.219 mm^3 (**Table 1**). The homogeneity of the spheroid size is reflected by a small standard deviation ranging from 0.002 to 0.034 mm^3 of the mean. We also observed that cell types such as MDA-MB-231, MDA-MB-468, MDA-MB-435, T-47D, SK-BR3, and MCF7-ADR formed spherical spheroids, with the *z* axis having a mean value of 102% of the *x*-/*y*-axis value, whereas MCF7 and MDA-MB-361 cells tended to exhibited a more elliptic structure in suspension culture, with the *z* axis being approximately 45% of the *x* and *y* axes.

Cell viability of spheroid cells

To investigate the accumulation and localization of dead cells in spheroids generated by centrifugation in rBM-supplemented medium, we analyzed MDA-MB-231 spheroids by performing a microscopic inspection of PI-labeled dead cells. As evident from **Figure 8A** and **B**, the rim of the spheroids consists of PI-negative, viable cells only. As early as 24 h, however, dead cells were detectable in the center region of the spheroid (**Fig. 8A**). The core region of PI-positive, dead cells increased significantly in 10-day-old spheroids (**Fig. 8B**).

Because the viability of cells in 3D culture might change after rBM-induced aggregate compaction, we compared the amount of viable cells in the spheroids grown with and without rBM after 1, 2, 3, 4, 6, and 10 days of culture. Spheroids were disintegrated into single cells, and viable versus apoptotic versus dead cell analysis was performed by annexin-V-fluos/PI staining and flow cytometric analysis. **Figure 8** shows typical examples of flow cytometric annexin-V-fluos/PI dot plots of MDA-MB-231 spheroids in the presence of 2.5% rBM after a 24-h (**Fig. 8C**) and a 10-day (**Fig. 8D**) culture period. The time kinetics of cell viability in 8 different breast cancer spheroids cultured with or without rBM is shown in **Figure 8E**. Except

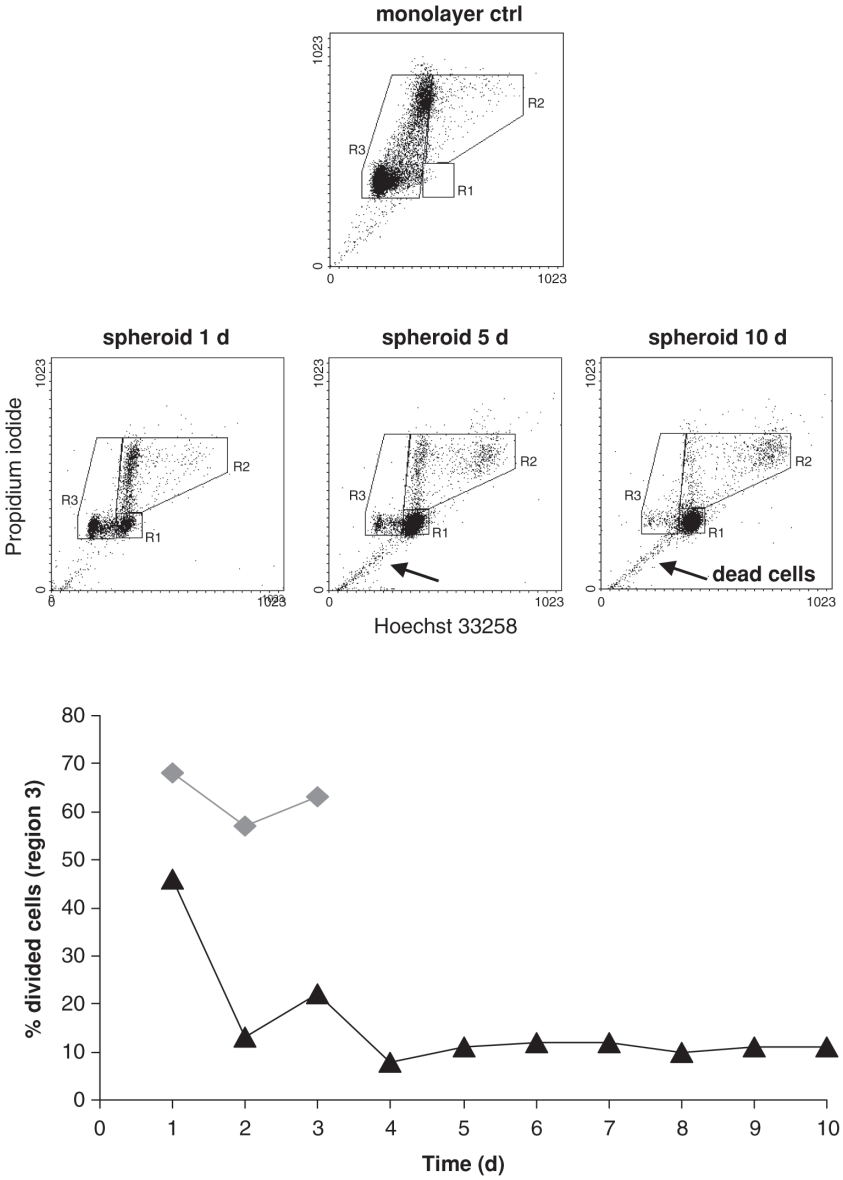

FIG. 5. Growth kinetics analysis of MDA-MB-231 cells using the dual-color flow cytometric BrdU/Hoechst 33258 quenching technique. The fluorescence-activated cell sorting (FACS) dot plots display a subconfluent monolayer culture as control culture and spheroids generated from 10,000 cells grown for 1, 5, and 10 days in suspension. The noncycling, arrested G1-phase fraction is located in R1, the slow proliferating cells in R2, and the divided cell fraction in R3. The bottom graph displays the quantitative proportion of divided MDA-MB-231 cells in monolayer cultures (gray squares) compared to the spheroid cultures (black triangles). The dot plots (8 spheroids pooled for analysis) are representative of the 2 independent experiments.

MDA-MB 231 and MDA-MB 468, the viability was not significantly altered regardless of whether cells were grown in the presence or absence of rBM. The cell viability in spheroids decreases at low rates continuously until a 6-day culture period, with a steep decrease thereafter in MCF7-ADR, MDA-MB 435, and MDA-MB 361 spheroids. Both MCF7 and T47-D cells, which generate tightly packed spheroids even in the absence of rBM, exhibit an initial higher death rate. rBM itself showed no significant toxic effects with any of the breast cancer cell lines when grown in 2D cultures (data not shown).

However, because there is still a significant proliferating cell fraction with the spheroids at each time point (**Fig. 5**), we investigated the alteration of the absolute number of viable cells. As a representative example, we investigated MDA-MB 231 spheroids and analyzed the total number of viable cells at the beginning and end of the culture period (for each time

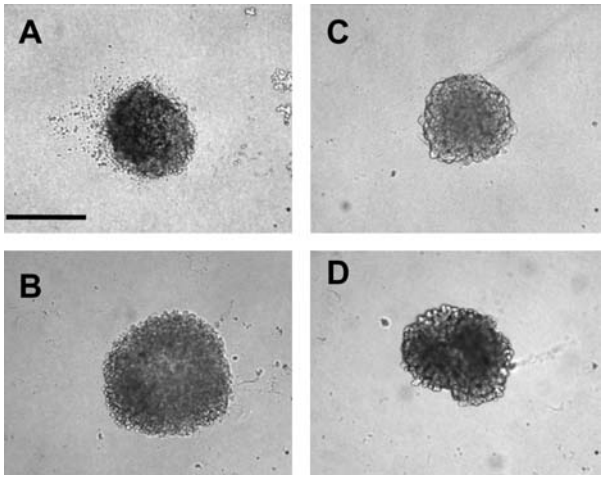

FIG. 6. Formation of spheroids from different breast tumor cell lines in poly-HEMA–coated, round-bottom, 96-well plates (5000 cells/well). Reconstituted basement membrane (2.5%) was added prior to the centrifugation step. (**A**) MDA-MB-468, (**B**) SK-BR3, (**C**) MDA-MB-435, and (**D**) MDA-MB-361. Size of black bar = 500 µm.

Table 1. Size Homogeneity of Single-Well Suspension Spheroids from Breast Cancer Cell Lines

	Mean Volume (mm^3)	*Mean Diameter (x × y) (mm)*
MDA-MB-231	0.039 ± 0.002	0.42 × 0.42
MDA-MB-468	0.084 ± 0.017	0.49 × 0.59
MCF7-ADR	0.129 ± 0.034	0.59 × 0.65
SK-BR-3	0.130 ± 0.015	0.61 × 0.64
MDA-MB-435	0.077 ± 0.012	0.51 × 0.54
MDA-MB-361	0.127 ± 0.027	0.51 × 0.73
MCF7	0.219 ± 0.032	0.71 × 0.79
T-47D	0.092 ± 0.026	0.51 × 0.6

The volume was calculated assuming an ideal sphere morphology from the geometric mean of 2 orthogonal diameters (mean ± SD of 8 spheroids; 5000 cells seeded per well, 24-h spheroid culture).

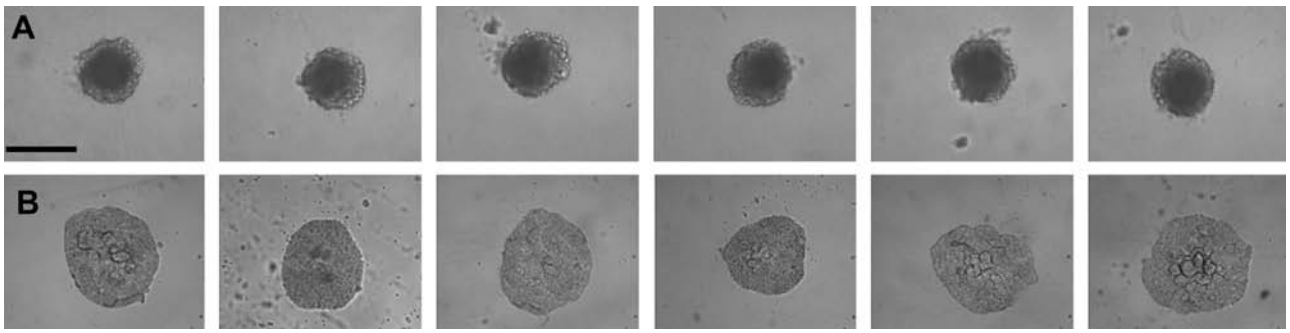

FIG. 7. Reproducibility of size and geometry of MDA-MB-231 and MCF7 spheroids growing as a single entity in individual wells of poly-HEMA–coated, round-bottom, 96-well plates (5000 cells/well). (**A**) MDA-MB-231 spheroids generated over 24 h in the presence of 2.5% reconstituted basement membrane (rBM) and (**B**) MCF7 spheroids generated without rBM. Size of black bar = 500 µm.

point, 4 pooled spheroids). Despite a decline of the percentage of viable cells from 80% (viable/total cells, 16,094/20,118) to 77% (viable/total cells, 25,470/33,078) to 64% (viable/total cells, 44,674/69,803) after a 1-, 3-, and 10-day culture period, respectively, it is evident that the total number of viable cells is even higher at the end of the culture period.

Suspension microplate spheroids from non–breast cancer cell lines

We tested the universal applicability of the microplate, single-well suspension spheroid generation in a wide range of non–breast cancer cell lines using poly-HEMA–coated, 96-well plates. As evident from **Figure 9**, HEK293 cells formed spheroids even in the absence of rBM (**Fig. 9A**, upper and lower row). In contrast, IGROV-1, A549, Colo 205, HepG2, and PC-3 cells form loose aggregates in 3D (**Fig. 9B-F**, upper row). However, rBM induces spheroid formation in all these cells lines, giving rise to compact single spheroids in individual wells (**Fig. 9**, lower row). **Table 2** summarizes the 3D morphological growth characteristics of the different cell lines tested, after a 24-h culture period. Nine of 12 cell lines tested forming aggregates in 3D culture can be transformed to compact spheroids using rBM.

DISCUSSION

Because of their 2D cellular assembly, the physiological phenotype of tumor cells in monolayer cultures differs significantly from their counterparts cultivated in 3D structures. One of the major physiological differences is the establishment of

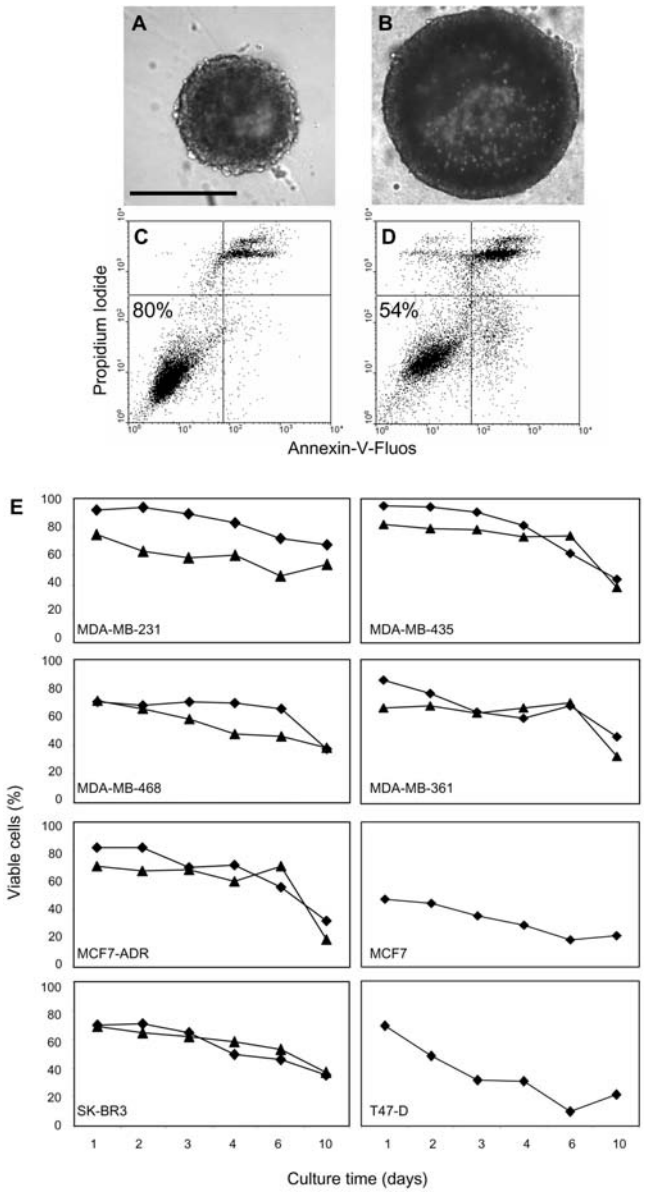

FIG. 8. Viability analysis of a cell grown in 3-dimensional culture. Ten thousand cells per well were seeded in poly-HEMA–coated, round-bottom, 96-well plates. (**A**, **B**) Microscopic analysis of dead cell propidium iodide (PI) staining in the core region of MDA-MB-231 spheroids cultivated in suspension with reconstituted basement membrane (rBM) for 1 and 10 days, respectively. Bar = 500 µm. (**C**, **D**) Flow cytometric annexin-V/PI analysis of MDA-MB-231 spheroids in rBM medium after a 1- (**C**) and 10-day (**D**) culture period. Quadrant assignment: lower left = viable cells; lower right = apoptotic, viable cells; upper right = apoptotic, dead cells, secondary necrosis; upper left = oncosis. (**E**) Cell viability of 8 breast cancer tumor cell lines in the absence (aggregates) or presence (spheroids) of 2.5% rBM. MCF7 and T47-D cells form spheroids spontaneously in the absence of rBM. Diamonds = without rBM; triangles = with rBM. The mean value of the number of viable cells for each time point was obtained from 2 independent experiments (each analysis was performed with 8 pooled spheroids). The deviation of individual values from the mean ranged from 0.7% to 16%.

Table 2. Aggregate-to-Spheroid Transformation Induced by Reconstituted Basement Membrane (rBM) in Non–Breast Cancer Cell Lines

		3-Dimensional Growth	
Origin	*Cell Line*	*Without rBM*	*With rBM*
Renal	UO-31	Spheroid	Spheroid
	HEK 293	Spheroid	Spheroid
Ovary	SK-OV-3	Aggregate	Spheroid
	IGR-OV-1	Aggregate	Spheroid
Lung	NCI-H40	Aggregate	Spheroid
	NCI-H322M	Spheroid	Spheroid
	A549	Aggregate	Spheroid
Prostate	PC 3	Aggregate	Spheroid
	LnCap	Aggregate	Spheroid
Colon	Colo 205	Aggregate	Spheroid
	SW-620	Aggregate	Spheroid
	HCT-15	Aggregate	Spheroid
Liver	Hep G2	Aggregate	Spheroid

The morphology of the spheroids was assessed microscopically by phase-contrast imaging before and after the supplementation of the medium with 2.5% rBM in poly-HEMA–coated, 96-well plates after a 24-h culture period.

molecule diffusion gradients in 3D cultures. Although the in vivo tumor complexity with numerous different cell types cannot be completely mimicked by spheroids, the tumor vessel distal regions can be simulated by multicellular tumor spheroids.[1]

Various culture techniques exist to generate in vitro spheroids in suspension.[25-29] However, they are not suitable for a standardized, rapid, and large-scale production of spheroids in a format needed for HT assays. Large numbers of spheroids can be generated by the liquid overlay and spinner flask method; however, the formation requires long cultivation times and the spheroids are heterogeneous in size. Importantly, the latter aspect increases the variation of the physiological response pattern because of different sizes of diffusion gradients of, for example, inhibitory/activating molecules, nutrients, or metabolites, which contributes to the variability of cell physiological and biochemical analyses. The growth of single cells in semisolid medium for spheroid generation also exhibits significant limitations: It is a colony formation and not a true spheroid assay, the culture periods are prolonged, and drug interaction studies are limited (e.g., no pulse chase experiments can be performed). Moreover, biochemical or cellular analyses require difficult recovery of spheroids from semisolid medium.

The method described in this report uses a rapid and simple protocol for reproducible large-scale spheroid production from a large number of tumor cell lines. Single spheroids of equal size and similar geometry can be generated in suspension in a 96-well format within 24 h of cultivation (**Fig. 7**). The spheroids generated in suspension by centrifugation retain typical spheroid characteristics such as stratified composition with viable cells in the rim and accumulation of necrotic/apoptotic cells in the center (**Fig. 8A, B**). Because the sub-G1 fraction of dead cells exclusively originates

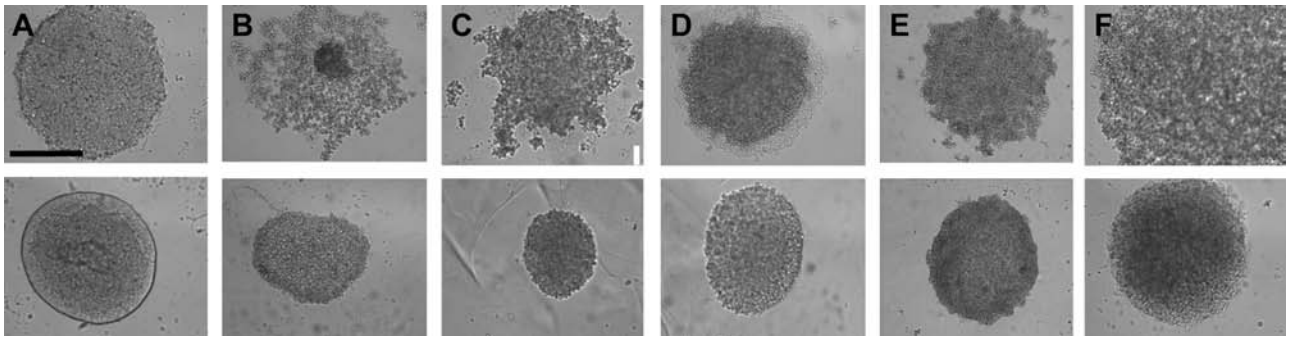

FIG. 9. Formation of spheroids from non–breast cancer cell lines using poly-HEMA–coated, round-bottom, 96-well plates (10,000 cells/well) in the absence (upper row) and presence (lower row) of 2.5% reconstituted basement membrane. Cell types: (**A**) HEK 293, (**B**) IGR-OV 1, (**C**) A549, (**D**) Colo 205, (**E**) HepG2 hepatoma, and (**F**) PC3. Size of black bar = 500 μm.

from the arrested G1-phase population (**Fig. 5**, arrows), it is obvious that the proliferating cell fractions are located mainly in the rim of the spheroids. In addition, stratification is also evident physiologically because the hypoxia-element-driven GFP expression in transfected tumor spheroids is found only within a ring limited by the rim of GFP-negative, nonhypoxic cells on the outside and dead, GFP-negative cells in the core region (data not shown).

Until now, we have generated single-well spheroids from 20 different tumor cell lines (**Tables 1** and **2**). Moreover, to mimic different stages of avascular tumor regions, the size of the spheroids can be adjusted to experimental needs by seeding different cell numbers per well prior to centrifugation: small spheroids containing primarily viable cells at the rim and core region and large spheroids harboring larger apoptotic/necrotic areas in the center.[12] Single spheroids can be established in 96-well plates with round- or conical-bottom wells, although centrifugation-dependent assembly of cells is slightly superior in conical-shaped wells. In addition, another major advantage of this suspension cell culture format of single spheroids is the ease of mechanical access and transfer to any plate or cell culture vessel format for further cultivation or analysis.

Because of diffusion limitations, death rates in spheroids are higher compared to 2D cell cultures. Compared to a cell viability of >95% of the 2D cultures, our xenograft 3D cell models exhibit either high initial death rates (MCF7, T47-D), low but constant death rates throughout the observation period (MDA-MB-231, MDA-MB-468, SK-BR3), or increased death rates at late time points of spheroid culture (MDA-MB-435, MDA-MB-361, MCF7-ADR). The rBM-induced compaction of the aggregates to spheroids did not increase the cell death rates in the breast cancer cell lines in general. Only in the MDA-MB-231 and MDA-MB-468 cell lines did we observe a 15% to 20% lower viability (**Fig. 8**). Because rBM did not affect cell viability in 2D cultures (data not shown), it can be applied as a nontoxic medium supplement in many different tumor cell lines to induce the transition from aggregates to spheroids (e.g., **Fig. 9**). Most likely, cell viability in the spheroid might be significantly affected by the 3D microenvironment of multicellular contacts such as the expression of tight junction molecules, which establish a diffusion barrier for nutrients and oxygen.[31]

A current limitation of the spheroid application in vitro is that numerous cancer cell lines do not form compact round spheroids in 3D.[1,20] For example, approximately half of the breast cancer cell lines tested in this study grew as aggregates of cells in 3D culture (**Fig. 1**), an architecture that differs from the compact in vivo cell-cell association of xenograft tumors. Fibronectin in its physiological dimeric conformation can induce aggregation, compaction, and subsequently spheroid formation in CHO cells.[32,33] Plasmin/urokinase from aged serum was shown to induce spheroid formation in suspension from MCF7 and ZR-75-1 cells.[34] However, the universal use of these proteins for spheroid compaction in a large number of cell lines has not been confirmed in our studies. Our supplementation experiments with different extracellular adhesion molecules indicate that the extract of rBM is superior over fibronectin, laminin, collagen, or proteoglycans alone or in combination (**Fig. 2**). The rBM-induced compaction of the aggregates occurred rapidly within 24 h without alteration of the cell culture medium viscosity. The more widespread application of our rBM-induced aggregate/spheroid transformation in suspension culture in single wells has been shown by its applicability to 9 of 12 non–breast tumor cell models (**Table 2**). Finally, because rBM is an extract of the basement membrane of a murine tumor, it also mimics more closely the in vivo xenograft growth environment of human tumor cells in mice.

In summary, with the method described, we provide a technique for spheroid generation from a large number of different tumor cell lines with several-fold advantages to previous reported methods: simple technique, rapid generation (24 h), production of large spheroid numbers (96-well plate format), single spheroids in suspension (easy accessibility), and morphological homogeneity

(little biological variability). Our microplate centrifugation technique requires only poly-HEMA–coated wells and, dependent on the cell type, rBM for generation of spheroids from aggregate-forming tumor cells. These suspension culture spheroids are applicable in an HT format for cellular and biochemical assays to analyze the impact of cytotoxic drugs, recombinant proteins, gene therapies, or the cellular microenvironment on proliferation, apoptosis, and gene expression in oncological relevant cell models.

REFERENCES

1. Mueller-Klieser W: Tumor biology and experimental therapeutics. *Crit Rev Oncol Hematol* 2000;36:123-139.
2. Mueller-Klieser W: Multicellular spheroids: a review on cellular aggregates in cancer research. *J Cancer Res Clin Oncol* 1987;113:101-122.
3. Pignatelli M, Bodmer WF: Integrin-receptor-mediated differentiation and growth inhibition are enhanced by transforming growth factor-beta in colorectal tumour cells grown in collagen gel. *Int J Cancer* 1989;44:518-523.
4. Sutherland RM, Sordat B, Bamat J, Gabbert H, Bourrat B, Mueller-Klieser W: Oxygenation and differentiation in multicellular spheroids of human colon carcinoma. *Cancer Res* 1986;46:5320-5329.
5. Mayer B, Klement G, Kaneko M, Man S, Jothy S, Rak J, et al: Multicellular gastric cancer spheroids recapitulate growth pattern and differentiation phenotype of human gastric carcinomas. *Gastroenterology* 2001;121:839-852.
6. Angello JC, Hosick HL: Glycosaminoglycan synthesis by mammary tumor spheroids. *Biochem Biophys Res Commun* 1982;107:1130-1137.
7. Grover A, Oshima RG, Adamson ED: Epithelial layer formation in differentiating aggregates of F9 embryonal carcinoma cells. *J Cell Biol* 1983;96:1690-1696.
8. Barcellos-Hoff MH, Aggeler J, Ram TG, Bissell MJ: Functional differentiation and alveolar morphogenesis of primary mammary cultures on reconstituted basement membrane. *Development* 1989;105:223-235.
9. Streuli CH, Bailey N, Bissell MJ: Control of mammary epithelial differentiation: basement membrane induces tissue-specific gene expression in the absence of cell-cell interaction and morphological polarity. *J Cell Biol* 1991;115:1383-1395.
10. Landry J, Freyer JP, Sutherland RM: A model for the growth of multicellular spheroids. *Cell Tissue Kinet* 1982;15:585-594.
11. Sutherland RM: Cell and environment interactions in tumor microregions: the multicell spheroid model. *Science* 1988;240:177-184.
12. Sutherland RM, Inch WR, McCredie JA, Kruuv J: A multi-component radiation survival curve using an in vitro tumour model. *Int J Radiat Biol Relat Stud Phys Chem Med* 1970;18:491-495.
13. Sutherland RM, Durand RE: Radiation response of multicell spheroids: an in vitro tumour model. *Curr Top Radiat Res Q* 1974;11:87-139.
14. Nederman T: Effects of vinblastine and 5-fluorouracil on human glioma and thyroid cancer cell monolayers and spheroids. *Cancer Res* 1984;44:254-258.
15. Olive PL, Banath JP, Evans HH: Cell killing and DNA damage by etoposide in Chinese hamster V79 monolayers and spheroids: influence of growth kinetics, growth environment and DNA packaging. *Br J Cancer* 1993;67:522-530.
16. Kobayashi H, Man S, Graham CH, Kapitain SJ, Teicher BA, Kerbel RS: Acquired multicellular-mediated resistance to alkylating agents in cancer. *Proc Natl Acad Sci U S A* 1993;90:3294-3298.
17. Ghosh S, Spagnoli GC, Martin I, Ploegert S, Demougin P, Heberer M, et al: Three-dimensional culture of melanoma cells profoundly affects gene expression profile: a high density oligonucleotide array study. *J Cell Physiol* 2005;204:522-531.
18. Klunder I, Hulser DF: Beta-galactosidase activity in transfected Ltk-cells is differentially regulated in monolayer and in spheroid cultures. *Exp Cell Res* 1993;207:155-162.
19. Kaaijk P, Troost D, Das PK, Leenstra S, Bosch DA: Long-term culture of organotypic multicellular glioma spheroids: a good culture model for studying gliomas. *Neuropathol Appl Neurobiol* 1995;21:386-391.
20. Kunz-Schughart LA, Freyer JP, Hofstaedter F, Ebner R: The use of 3-D cultures for high-throughput screening: the multicellular spheroid model. *J Biomol Screen* 2004;9:273-285.
21. Myrdal S, Foster M: Time-resolved confocal analysis of antibody penetration into living, solid tumor spheroids. *Scanning* 1994;16:155-167.
22. Torisawa YS, Takagi A, Shiku H, Yasukawa T, Matsue T: A multicellular spheroid-based drug sensitivity test by scanning electrochemical microscopy. *Oncol Rep* 2005;13:1107-1112.
23. De Witt Hamer PC, Jonker A, Leenstra S, Ruijter JM, Van Noorden CJ: Quantification of viability in organotypic multicellular spheroids of human malignant glioma using lactate dehydrogenase activity: a rapid and reliable automated assay. *J Histochem Cytochem* 2005;53:23-34.
24. Bartholoma P, Impidjati, Reininger-Mack A, Zhang Z, Thielecke H, Robitzki A: A more aggressive breast cancer spheroid model coupled to an electronic capillary sensor system for a high-content screening of cytotoxic agents in cancer therapy: 3-dimensional in vitro tumor spheroids as a screening model. *J Biomol Screen* 2005;10:705-714.
25. Santini MT, Rainaldi G: Three-dimensional spheroid model in tumor biology. *Pathobiology* 1999;67:148-157.
26. Carlsson J, Yuhas JM: Liquid-overlay culture of cellular spheroids. *Recent Results Cancer Res* 1984;95:1-23.
27. Sutherland RM, Durand RE: Growth and cellular characteristics of multicell spheroids. *Recent Results Cancer Res* 1984;95:24-49.
28. Moscona A: Rotation-mediated histogenetic aggregation of dissociated cells: a quantifiable approach to cell interactions in vitro. *Exp Cell Res* 1961;22:455-475.
29. Kelm JM, Timmins NE, Brown CJ, Fussenegger M, Nielsen LK: Method for generation of homogeneous multicellular tumor spheroids applicable to a wide variety of cell types. *Biotechnol Bioeng* 2002;83:173-180.
30. Omerod MG, Kubbies M: Cell cycle analysis of asynchronous cell populations by flow cytometry using bromodeoxyuridine label and Hoechst-propidium iodide stain. *Cytometry* 1992;13:678-685.
31. Hoevel T, Macek R, Swisshelm K, Kubbies M: Reexpression of the TJ protein CLDN1 induces apoptosis in breast tumor spheroids. *Int J Cancer* 2004;108:374-383.
32. Robinson EE, Zazzali M, Siobhan AC, Ramsey AF: a5β1 integrin mediates strong tissue cohesion. *J Cell Sci* 2002;116:377-386.
33. Robinson EE, Ramsey AF, Siobhan AC: Fibronectin matrix assembly regulates a5β1-mediated cell cohesion. *Mol Biol Cell* 2004;15:973-981.
34. Chun MH: Plasmin induces the formation of multicellular spheroids of breast cancer cells. *Cancer Lett* 1997;117:51-56.

Address reprint requests to:
Manfred Kubbies, Ph.D.
Pharmaceutical Research Oncology
Roche Diagnostics GmbH
Nonnenwald 2
82377 Penzberg, Germany

E-mail: manfred.kubbies@roche.com